

First observation of muonic hyperfine effects in pure deuterium

P. Kammel, W. H. Breunlich, M. Cargnelli, H. G. Mahler, and J. Zmeskal
Österreichische Akademie der Wissenschaften, Boltzmanngasse 3, A-1090 Vienna, Austria

W. H. Bertl

*Laboratorium für Hochenergiephysik der Eidgenössischen Technischen Hochschule Zürich,
 Schweizerisches Institut für Nuklearforschung, CH-5234 Villigen, Switzerland*

C. Petitjean

Schweizerisches Institut für Nuklearforschung, CH-5234 Villigen, Switzerland

(Received 17 March 1983)

We discovered a strong hyperfine dependence of the resonant formation process of $d\mu d$ mesomolecules, while detecting neutrons from muon-catalyzed fusion in pure deuterium gas at 34 K. This new effect enabled us to observe directly transitions between hyperfine states of the μd atom for the first time and to determine an accurate experimental value for this transition rate. Our analysis demonstrates the importance of hyperfine effects for the quantitative understanding of the mechanism of resonant $d\mu d$ formation. Moreover, this experiment indicates that the resonant formation process is a powerful tool for a refined spectroscopy of $d\mu d$ bound states. Finally, the detailed knowledge about mesoatomic and mesomolecular processes obtained in this work provides valuable information for the analysis of experiments on the elementary muon-capture process in deuterium.

I. INTRODUCTION

Mesoatomic and mesomolecular processes, which are induced by negative muons stopping in a mixture of hydrogen isotopes, have been the subject of numerous investigations for over 20 years. However, knowledge about hyperfine (hf) effects in these muonic hydrogen systems remained surprisingly scarce. This lack of information contrasts with the obvious importance of hf effects. The following discussion will be limited to the case of deuterium. There, it was repeatedly¹⁻³ pointed out that the interpretation of the two existing experiments⁴ on the elementary weak capture process



relies heavily on assumptions about the time distribution of the hf states of the μd atoms. The pronounced spin dependence of this semileptonic process is a well-known consequence of the $(V-A)$ structure of weak interactions.

In spite of considerable theoretical and experimental efforts it was not possible to settle the question of the population of μd hf states. In our present work we investigated time and energy spectra of neutrons emitted from the fusion reaction



by using a target filled with pure cold deuterium gas. By this method we succeeded in observing directly hf transitions for the first time and in determining experimentally the populations of the hf states of muonic deuterium.

Besides their importance for the basic muon-capture reaction (1) new interest in mesomolecular processes originates from the recent discovery of a resonance mecha-

nism in the formation of the $d\mu d$ molecules.^{5,6} The experimental investigation of this remarkable mechanism represents an excellent test of the theoretical understanding of the three-body Coulomb interaction among particles of comparable masses. Moreover, an analogous mechanism, which has been predicted for a mixture of deuterium and tritium, greatly enhances the expected rates for molecular $d\mu t$ formation, thus yielding a large number of fusion reactions catalyzed by a single muon. This new effect even encouraged speculations on possible applications in energetics.⁷ Our experiment points out that hyperfine effects lead to dramatic changes in the molecular formation rates in deuterium. This discovery clearly demonstrates the importance of hf effects for a detailed understanding of this resonant formation process.

Preliminary results of our experiment have been published in Refs. 3, 8, and 9. In this paper the final results will be presented together with a detailed description of the experiment and the various conclusions.

II. ATOMIC AND MOLECULAR PROCESSES

As there exist several review articles on this subject,^{3,10,11} we concentrate on the open problems and the recent developments in this field.

A. Hyperfine transition

Muonic deuterium atoms in their ground state are formed in two hyperfine states, the $F = \frac{3}{2}$ and the $F = \frac{1}{2}$ state, according to their statistical weights (F is the total spin of μd atoms). These small neutral systems scatter with high elastic cross sections¹⁰ against the nuclei of the neighboring molecules, which results in a fast thermaliza-

tion compared to the muon decay rate $\lambda_0=0.455 \times 10^6$ s⁻¹. In addition, due to resonant charge exchange, inelastic hyperfine transitions take place:

$$\mu d (F = \frac{3}{2}) + d \rightleftharpoons \mu d (F = \frac{1}{2}) + d . \quad (3)$$

As soon as the kinetic energy of the μd atoms approaches the hf splitting energy $E_{\text{hf}}=49$ meV between the $F=\frac{3}{2}$ and the $F=\frac{1}{2}$ state, this process changes the original statistical distribution of μd hf states, leading to a depopulation of the $F=\frac{3}{2}$ state with the rate $\lambda_d^{\mu d}$ (unlike our previous publications,^{3,9} where rates were normalized to liquid-deuterium density of 4.84×10^{22} cm⁻³, all rates given in this work refer to liquid-hydrogen density $c_0=4.2 \times 10^{22}$ cm⁻³).

Contrary to the case of isotopically pure ¹H, where all μp atoms reach the lower hyperfine state with a very fast rate compared to the muon decay rate λ_0 , already the first theoretical calculation¹² had indicated that in deuterium (with a density of a few percent of c_0) the hf transition rate is comparable to λ_0 . Therefore, during the whole lifetime of the muon, the time distribution of muonic hf states remains sensitive to the value of $\lambda_d^{\mu d}$.

As no hf-dependent mesomolecular processes in pure deuterium were known before this work, experimental searches concentrated on hydrogen contaminated with a few percent deuterium. For such a mixture a sensitivity of the yield of fusion gamma rays (following $p\mu d$ formation)

to the spin state of the μd atoms has already been predicted in 1960 (Wolfenstein-Gershtein effect).¹² This effect was investigated with various techniques in liquid as well as in gaseous targets.¹³⁻¹⁶ As can be seen in Table I (first and second column) all experimental results published before 1979 agree well with the old theoretical result.¹² Remarkably, more recent calculations of Ponomarev *et al.*,^{18,19} predicting a much larger value of $\lambda_d^{\mu d}$, were clearly excluded by the experimental data.

However, a refined analysis of the experiments with liquid H-D mixtures indicates that this conclusion is misleading. In agreement with theoretical estimates (no detailed calculations exist)¹⁰ the spin-flip process

$$\mu d (F = \frac{3}{2}) + p \rightarrow \mu d (F = \frac{1}{2}) + p , \quad (4)$$

which proceeds with the rate $\lambda_p^{\mu d}$, was neglected in the original analyses of these experiments. This leads to a poor agreement between the old experiments on fusion yields in liquid H-D mixtures and the theoretical predictions.³ Only recently we have performed a new, sufficiently accurate measurement of the absolute yield of fusion gamma rays. This experiment¹⁶ suggests an unexpectedly²⁰ high value of $\lambda_p^{\mu d} \geq 4 \times 10^6$ s⁻¹ (for a discussion of preliminary results of this experiment we refer to Refs. 3 and 16). Concerning the value of $\lambda_d^{\mu d}$, which is a main topic of our present paper, the analysis mentioned above indicates that—due to the additional hf transition induced

TABLE I. Hyperfine transition rate $\lambda_d^{\mu d}$.

Reference	$\lambda_d^{\mu d}$ (10^6 s ⁻¹) (normalized to density of liquid H ₂)			
	Theoretical results	Experimental results		Experiments in pure D ₂ No assumptions about $\lambda_p^{\mu d}$ necessary
		Original analysis assuming $\lambda_p^{\mu d} \sim 0$	Experiments in H-D mixture Preliminary reanalysis from Ref. 3 assuming $\lambda_p^{\mu d} = (4 \pm 2.5) \times 10^6$ s ⁻¹	
Dubna ^a (1961)	7			
Chicago ^b (1963)		7 ⁱ	~ 35	
Columbia ^c (1963)		7 ⁱ	~ 35	
Dubna ^d (1970)	47			
Dubna ^e (1976)		< 15 ^j		
Vienna-SIN ^f (1978)			35 ± 20	
Dubna ^g (1979)	46			
Dubna ^h (1981)				> 40 ^{i,k}
This work Vienna-SIN				37.0 ^{+1.3} _{-1.7}

^aReference 12.

^bReference 13.

^cReference 14.

^dReference 18, result calculated for collision energy of about 4 meV.

^eReference 15.

^fReference 16.

^gReference 19, result calculated for collision energy of 50 meV. According to the energy dependence of $\lambda_d^{\mu d}$ (Ref. 18), this value should be reduced by about 27% at a collision energy of 4 meV.

^hReference 17.

ⁱThe authors found no contradiction to Ref. 12 (theory 1961), and therefore, accepted this result.

^jLimit for 90% confidence level.

^kNote, however, the ambiguity in the interpretation of this result discussed in Ref. 17.

by process (4)— $\lambda_d^{\mu d}$ is determined only within large errors from experiments in liquid H-D mixtures (compare third column of Table I).

The work of the last years thus shows that some seemingly well-established limits for $\lambda_d^{\mu d}$ have to be reconsidered. No accurate experimental result for $\lambda_d^{\mu d}$ exists. Experiments are even inconsistent among each other. This situation clearly underscores the necessity of an independent and accurate determination of $\lambda_d^{\mu d}$.

B. Formation of $d\mu d$ molecules

Another process, which deserves special interest is the molecular formation



(with the rate λ_{dd}). In addition to the Auger process, responsible for the ordinary formation of muonic mesomolecules, a resonance mechanism takes place in pure deuterium. In this process the binding energy of the $d\mu d$ molecule is transferred into the excitation of the whole mesomolecular complex according to the following scheme:



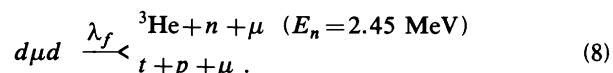
As the binding energy of muonic molecules is usually of the order of some 100 eV, the crucial point for this mechanism is the existence of a weakly bound $J=1, \nu=1$ state of the $d\mu d$ molecule with a binding energy ϵ_{11} below the D_2 dissociation limit of ~ 4.5 eV (J is the rotational and ν the vibrational quantum number).

After the first suggestion of such a mechanism in 1967,²¹ it took a lot of elaborate theoretical work by Ponomarev and co-workers to prove the existence of this state and to calculate its energy with an estimated error of some meV in 1982.²² Compared to the typical energy scale of muonic atoms, this error is about 10^{-6} of the muonic Rydberg, which is a remarkable theoretical accuracy.

Experimental physics now has a unique and even more precise possibility of testing these three-body bound-state calculations: After thermalization the kinetic energies of μd atoms follow a Maxwell distribution according to the target temperature. Resonant formation of $d\mu d$ molecules is only possible if the kinetic energy of the μd atom exactly equals the resonance energy ϵ_0 (compare Fig. 1), where

$$\epsilon_0 = \epsilon_{11} - \Delta E \quad (7)$$

(ΔE is the energy difference between the D_2 ground state and the excited rotational, vibrational state of the complex $[(dd\mu)dee]$ molecule. Compare Ref. 6 for details.) An ideal monitor is provided by the well-known spontaneous nuclear fusion process, whose sizable probability is due to the small distance of nuclei (~ 500 fm) bound in the $d\mu d$ molecule:



By measuring the temperature dependence of the yield of fusion neutrons between 120 and 380 K the resonance

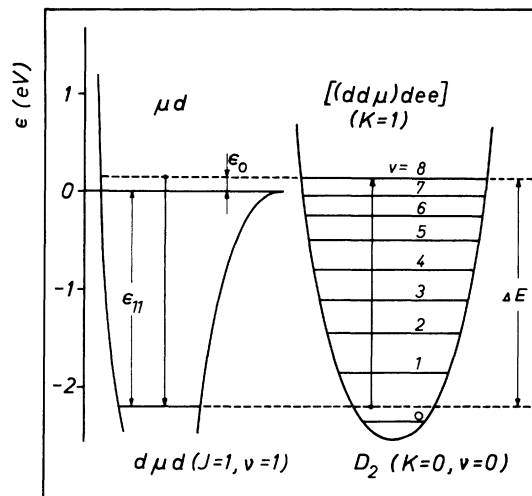


FIG. 1. Energy levels for resonant molecular formation (from Ref. 6). At the resonance condition the energy gain for the transition from the scattering μd state to the $d\mu d$ molecular level with $J=1, \nu=1$ is spent on the excitation of the whole complex $[(d\mu d)dee]$. Results of this work suggest that the transition proceeds to the $\nu=7$ level (instead of $\nu=8$).

mechanism was verified in an experiment performed in 1977,⁵ and a resonance energy ϵ_0 of 53 meV was extracted.⁶ This corresponds to an energy of $\epsilon_{11} = -2.196 \pm 0.003$ eV, with an impressive experimental error of $\sim 10^{-6}$ of the muonic Rydberg. Comparison of this experimentally determined value with the theoretical result $\epsilon_{11} = -1.96$ eV shows a discrepancy of -0.24 eV (compare Ref. 6).

We want to point out the following problems in this important experimental test of three-body bound-state calculations:

(i) Above all, no hyperfine effects were taken into account in the analysis⁶ of experiment,⁵ although the hyperfine splitting energies of the μd atom and the $d\mu d$ molecule are both comparable to the resonance energy.

(ii) The existence of D_2 molecules in higher rotational levels, which are expected to dominate at 300 K, was omitted in the analysis. As these states are separated by several meV, various $E1$ transitions with different resonance energies are possible.²³

Thus a resonance behavior of λ_{dd} has been established beyond doubt in Ref. 5. Our discussion, however, shows that this investigation of the resonant molecular formation mechanism is of a qualitative nature only.

III. EXPERIMENT

A. Method

The general sequence of electromagnetic and strong interaction processes, which take place after stopping negative muons in pure deuterium gas of density c is displayed in Fig. 2 (the gas density c is defined as the D_2 -gas density normalized to c_0). In addition the muon may decay at any

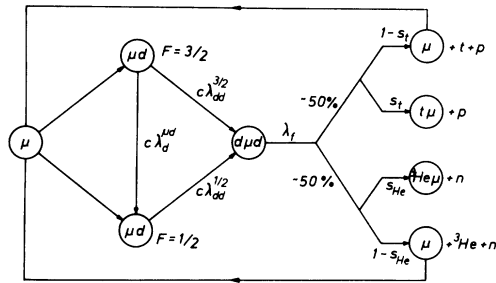


FIG. 2. General sequence of muon induced processes in deuterium. Splitting of the molecular formation according to the hf splitting of the atomic ground state was discovered in this experiment. hf structure of the participating molecular state was omitted for simplicity.

point on the diagram with the rate λ_0 . In particular we want to emphasize the distinction between $\lambda_{dd}^{1/2}$ and $\lambda_{dd}^{3/2}$, the molecular formation rates from the $F = \frac{1}{2}$ and $F = \frac{3}{2}$ μd hyperfine states, respectively. This distinction is taken into account for the first time and was omitted in all previous work on this subject, especially in the analysis of the resonant $d\mu d$ formation.⁶

If one considers the high value of the fusion rate²⁴ $\lambda_f \sim 10^9 \text{ s}^{-1}$ compared to all other rates, it becomes clear from Fig. 2 that the observation of fusion neutrons is a sensitive tool in investigating the processes leading to $d\mu d$ formation. Therefore, we measured time and energy spectra of fusion neutrons, emitted from reaction (2), after muon stop. As no theoretical predictions were available about hyperfine effects in 1979, the problem was to estimate the suitable temperature and density where hf effects should show up. We chose a temperature range around 34 K, which had not been investigated before. Low gas density ($\leq 5\%$ of liquid density) was necessary, to ensure that the effective hf transition rate $c\lambda_{dd}^{\mu d}$ was slow enough to be experimentally observable.

B. Experimental arrangement

A schematic drawing of the apparatus employed in this experiment is given in Fig. 3. The target was a cylindrical copper vessel (of cross-sectional diameter 14 cm, length 20 cm, walls 0.2 cm) placed inside a vacuum chamber, which provided the necessary thermal insulation. Silver foils were used as target windows (thickness 0.5 mm) and also covered the inner surface of the target cylinder. This ensured a fast decay ($\tau_{Ag} \sim 85 \text{ ns}$) of muons stopping in the target walls. The performance of the target, the cooling, and the temperature stabilization will be published elsewhere. The target gas was purified with a palladium filter. The level of impurities in the target gas, which is always a critical parameter for mesomolecular processes in hydrogen, was below 10^{-1} ppm.

The muon stops were defined by a beam telescope consisting of three plastic scintillators (1,2,3 in Fig. 3). Detector 2, which had a circular entry hole of 6 cm diameter in its center, was used as a prompt veto for the stop signal. Thus a well-defined beam spot was obtained. In addition,

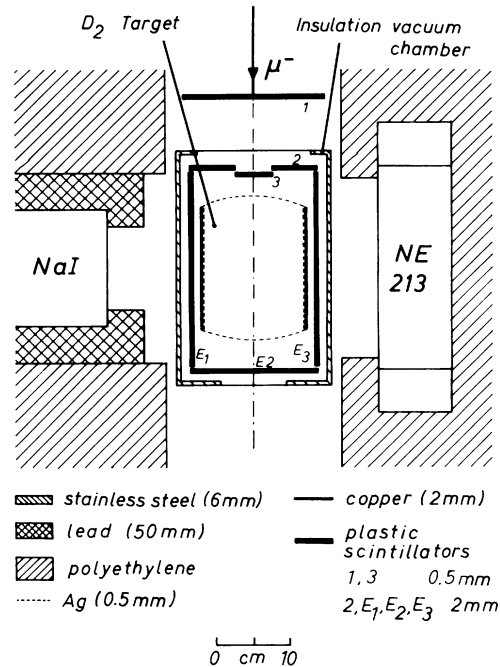


FIG. 3. Experimental arrangement.

electrons passing through the light guide of detector 2 were rejected.

Electrons from muon decay were detected by seven plastic scintillators (detector 2 and detectors E_i , $i=1,6$). Contrary to standard arrangements, these detectors were placed inside the insulation vacuum chamber. This design proved to be of particular importance for our experiment (compare Sec. IV), because it reduced electron scattering, and ensured efficient electron detection ($\Omega/4\pi \sim 90\%$).

Neutrons were detected by a large Nuclear Enterprises NE-213 liquid scintillation detector ($28 \times 14 \times 10 \text{ cm}^3$). Both ends of the detector volume were viewed by Philips XP-2041 photomultipliers. By adding the signals of both sides a homogeneity of $< 3\%$ within the whole large volume was obtained.²⁵ The effective solid angle for neutron detection was about 6%, the intrinsic efficiency for 2.5-MeV neutrons amounted to about 40% (using a lower energy threshold of 345-keV equivalent electron energy).⁸ The NaI detector was used for background studies only (see Sec. IV A).

C. Electronics

The electronics for the different measurements are best explained with the help of the simplified schematic diagram in Fig. 4. The *muon stop signal* was defined by $1 \cdot 2 \cdot 3 \cdot \sum E_i$, indicating a beam particle stopping in the target region. Because of the high intensity of muon stops ($\sim 6 \text{ kHz}$) the physical start-stop sequence had to be inverted to prevent high deadtime losses due to a large start rate of the time-to-amplitude converters (TAC). This inversion was achieved naturally since a pile-up gate was used for the muon stop signal. This module²⁶ rejected all muon stops, accompanied by another beam particle entering the experimental area (detected by detector 1) within 7

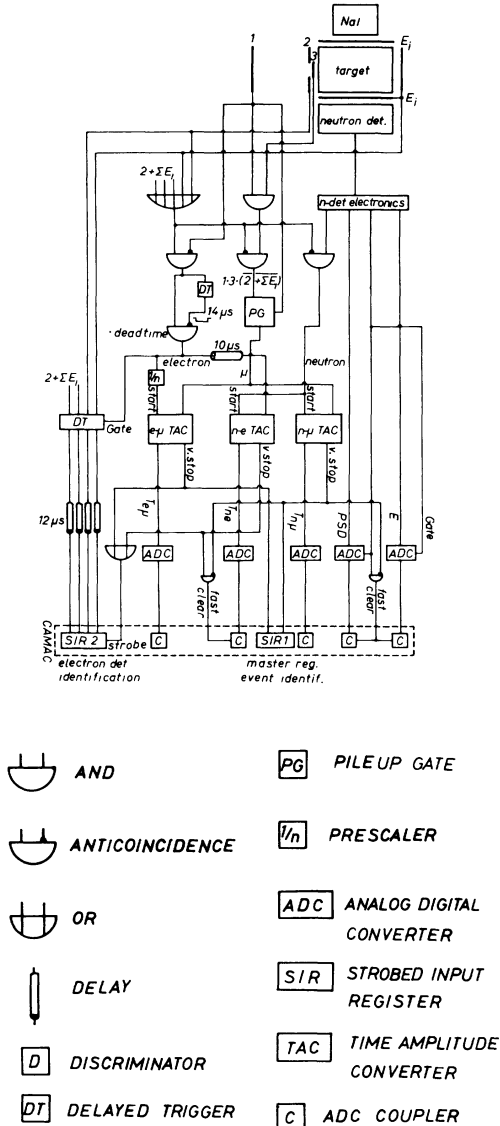


FIG. 4. Simplified block diagram of the electronics. NaI electronics was omitted for simplicity.

μ s before and after. This condition reduced the accidental neutron background substantially and also avoided pile-up distortions of the time spectra. As this pile-up information is available only 7μ s after the original signal, the μ signal, which is the muon stop signal free from pile-up events, appeared after a correspondingly long delay and could be used directly as the stop signal for the various TAC's (Fig. 4).

For two sorts of events the following information was recorded on tape by a PDP 11/34 computer (Digital Equipment Corp.).

Neutral events:

The pulse height, produced by recoil protons in the NE-213 detector (E).

The pulse shape information,²⁷ discriminating between gammas and neutrons (PSD).

The time between a neutron signal and the delayed μ signal ($T_{n\mu}$). The neutron time signal was obtained by a

constant fraction discriminator and included a prompt charged particle veto from the $(2 + \sum E_i)$ detectors (width ± 70 ns). Its rate was further reduced by requiring hardwired PSD and energy cuts.

The time between a neutron signal and the electron signal in the plastic detectors (T_{ne}). For the electron signal $(2 + \sum E_i) \cdot \bar{I}$ a fixed deadtime (Fig. 4) of 14μ s was introduced.

A register indicated which electron detector had fired.

Decay electron events:

The time between an electron signal and the μ signal ($T_{e\mu}$).

A register indicated which electron detector had fired.

If the various ADC signals did not complete one of the events defined above, a fast clear of the ADC couplers was possible. This arrangement avoided the long CAMAC deadtime ($\sim 500 \mu$ s).

D. Measurements

The measurements were performed at SIN at the μ E4 beam line using a $50 \text{ MeV}/c \mu^-$ beam. For this low momentum beam an excellent range width of $100 \text{ mg}/\text{cm}^2$ FWHM (full width at half maximum) was obtained.

Beam tuning. At the μ E4 area it was possible to choose the optimal beam momentum by adjusting the momentum defining magnet. Usually the μ^- beam is tuned to achieve the highest muon stop rate. As the mass of the entrance windows ($300 \text{ mg}/\text{cm}^2$) exceeds the mass of the gas target ($72 \text{ mg}/\text{cm}^2$ at $2.4\% c_0$) such a procedure would be insensitive in our case, even favoring stops in the entrance windows. To improve our information about the muon stopping distribution the large differences in the lifetimes of muons stopping in the windows or in the gas of the target were used.

Therefore decay electron events were measured for various beam momenta. The intensities of the λ_0 decay component (characteristic for stops in hydrogen), which were determined from the $T_{\mu e}$ time spectra of the E_i detectors, then are nearly insensitive to solid angle effects and correspond directly to the number of muons stopping in the D_2 gas.

Data runs. Data were taken in pure D_2 gas for different densities and about 34 K temperature (Table II). In addition background studies with μ^+ and with xenon fillings were performed. During the data runs the decay electron events were suppressed by a factor of 300.

IV. DATA ANALYSIS

A. Selection of fusion neutrons

In a first step neutral events were separated from the intense bremsstrahlung background (due to electrons from muon decay) by applying proper PSD and energy cuts ($345\text{--}870 \text{ keV}$ electron energy scale). The remaining events consisted of (i) fusion neutrons [process (2)], (ii) accidental neutrons, (iii) capture neutrons [process (1)], (iv) capture neutrons due to muon stops in the target walls, (v) capture neutrons due to muons transferred to gas impurities, (vi) silver capture neutrons due to μd atoms diffusing

TABLE II. Summary of data run conditions.

Density (% of c_0)	Temperature (K)	μ signals	Stops in D_2 per μ signals
9.53 ± 0.19	32.0 ± 0.5	3.08×10^8	~ 0.85
4.78 ± 0.10	34.7 ± 0.5	5.44×10^8	~ 0.67
2.35 ± 0.05	34.9 ± 0.5	2.84×10^8	~ 0.40

to the target walls, and (vii) photoneutrons produced by bremsstrahlung.

Backgrounds (iv)–(vii) are well known from experiments on nuclear muon capture⁴ in hydrogen and are listed here for completeness only. They are estimated to produce some ten percent corrections to the neutrons coming from the deuterium capture process (iii). These estimates were quantitatively checked for background (iv) (Xe filling), (vi) (detection of x rays from muonic silver with a NaI detector), and (vii) (μ^+ runs). The remaining open problem was the clear discrimination between fusion (i) and capture (iii) neutrons, which was a major difficulty, because both rates are of comparable magnitude in our experimental conditions. An accurate subtraction of capture neutrons was impossible, because the rate of this process is experimentally unknown within a factor of 2 (compare Ref. 3).

However, Fig. 2 shows that the fusion process is characterized by the survival of the muon, acting as a catalyzer only. On the contrary the muon vanishes in processes (iii)–(vii). Figure 5 displays the strong correlation between the detected neutrons and electrons in the T_{ne} time spectrum. By requiring a delayed coincidence between a neutron and the decay electron from the recycled muon²⁸ it was possible to suppress all capture events by more than one order of magnitude, reducing background (iii)–(vii) to a 3% correction.⁸ Making use of this very efficient method to get clean fusion spectra one has to keep in mind that it leads to a considerable deformation of the originally flat background (ii) of accidental neutrons.²⁹ This effect is caused mainly by the time dependence of the probability for a delayed coincidence between a decay electron and an uncorrelated neutron. A careful discussion⁸ shows that it is possible to reduce this variation of the accidentals to less than 3%, by choosing proper time windows for the delayed coincidence interval (Fig. 5). This method for correct accidental subtraction is illustrated in Fig. 6 for a typical run.

B. Determination of the electron detector efficiency

It is worthwhile mentioning that the coincidence condition described in the preceding section gives rise to an elegant method to determine the overall efficiency of the plastic scintillators to detect electrons coming from the extended target region. Owing to their characteristic time dependence (see next section) the number of fusion neutrons in the fast time component of the $T_{\mu n}$ spectra can be clearly identified with and also without the delayed electron coincidence condition. The corresponding numbers

are N^c and N , respectively. As a first approximation (for details see Ref. 8)

$$N^c = N\epsilon_e, \quad (9)$$

where ϵ_e is the efficiency of the $(2 + \sum E_i)$ plastic scintillators to detect the muon decay within the neutron electron coincidence interval. Thus an *in situ* overall electron efficiency was obtained. As a result of this new method the ratio of muons stopping in the target gas to the total muon stop rate was calculated (Table II) by dividing the measured decay electron yields in the $T_{e\mu}$ spectra by the simultaneously measured efficiencies ϵ_e . The full advantage of this new normalization method was not exploited in this experiment, since no absolute normalization was needed.

C. Analysis of corrected fusion events

The time spectra of fusion neutrons after muon stop, which are obtained after the subtraction of the accidental background, are displayed in Fig. 7 for the different gas densities. Obviously these spectra exhibit two decay components in contrast to the single exponential slope expected from the existing literature. Both time components are clearly identified as due to the fusion process, because the

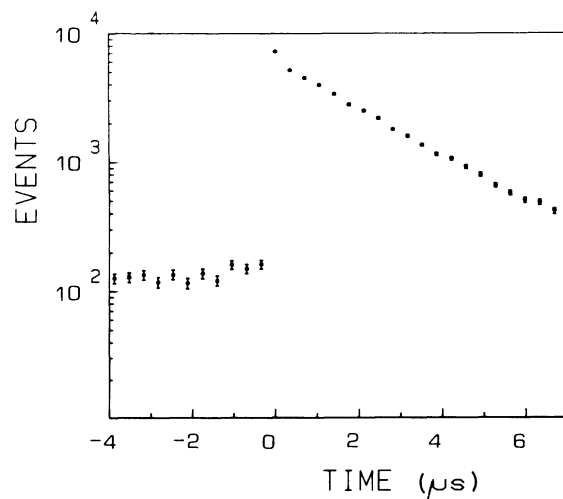


FIG. 5. Neutron-electron correlation (spectrum T_{ne}). Strong correlation between fusion neutrons and electrons from muon decay is shown by the slow decay component on top of flat background of uncorrelated events. Additional prompt correlation (spike at time zero) is mainly due to photoneutrons [background (vii)]. During the data runs it was suppressed by a charged particle veto (described in Sec. III C).

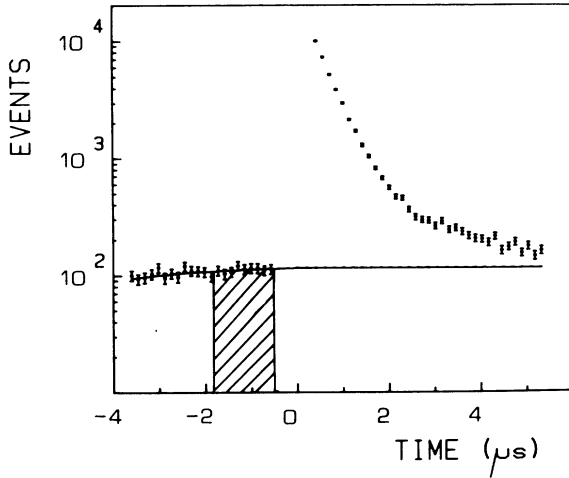


FIG. 6. Raw spectrum of fusion neutrons after muon stop (to reduce the counting rate events in the first 300 ns after muon stop were not recorded on tape). Time dependence of the distribution of accidentals, induced by the coincidence condition on the T_{ne} spectra ($\pm 6.8 \mu s$), was calculated (Ref. 8). Hatched region prior to the muon stop was used to normalize this calculated curve to the measured spectrum.

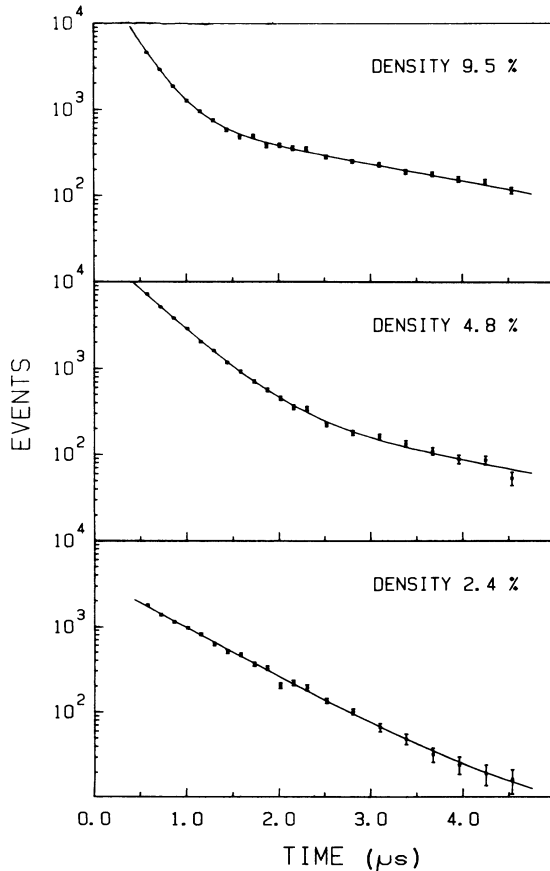


FIG. 7. Time spectra of fusion neutrons after muon stop (bin width $0.144 \mu s$). The solid curves result from a fit in the time range $0.6 < t < 5 \mu s$. Gas density is normalized to liquid-hydrogen density.

characteristic shape of the pulse height spectrum for fusion neutrons in the NE-213 scintillator (Fig. 8) does not change in the analyzed time interval ($0.6 \leq T_{\mu n} \leq 5 \mu s$). Thus we conclude that in our experimental conditions the μd atoms exist in both hf states with strongly differing molecular formation rates. Due to the hyperfine transition with the rate $c\lambda_d^{\mu d}$ the upper $F = \frac{3}{2}$ state disappears much faster than the lower $F = \frac{1}{2}$ state. The fast component in the observed spectra of fusion neutrons (Fig. 7) is naturally explained by the decay of this $F = \frac{3}{2}$ state, the high neutron intensity indicating a large rate $\lambda_{dd}^{3/2}$ for the molecular formation from this atomic hf state. The slow component with a decay constant equal to λ_0 then is due to the much lower $d\mu d$ formation rate $\lambda_{dd}^{1/2}$ for the $F = \frac{1}{2}$ state of the μd atom.

Following this new idea of distinct hyperfine formation rates λ_{dd}^F of the $d\mu d$ molecule (according to Fig. 2) a system of differential equations is derived for the population of the hf states of the μd atom ($n_{1/2}$ and $n_{3/2}$) and the population of the $d\mu d$ molecule (n_{dd}). (The notations are explained in Fig. 2. s is the integral sticking probability per fusion process.³⁰ s equals $\frac{1}{2}s_{He}$, because due to the high stripping probability the sticking of muons to tritium can be neglected.) Thus

$$\begin{aligned} \frac{dn_{1/2}}{dt} &= -(\lambda_0 + c\lambda_{dd}^{1/2})n_{1/2} + c\lambda_d^{\mu d}n_{3/2} + \frac{1}{3}\lambda_f(1-s)n_{dd}, \\ \frac{dn_{3/2}}{dt} &= -(\lambda_0 + c\lambda_d^{\mu d} + c\lambda_{dd}^{3/2})n_{3/2} + \frac{2}{3}\lambda_f(1-s)n_{dd}, \end{aligned} \quad (10)$$

$$\frac{dn_{dd}}{dt} = c\lambda_{dd}^{1/2}n_{1/2} + c\lambda_{dd}^{3/2}n_{3/2} - (\lambda_0 + \lambda_f)n_{dd}.$$

The observed yield of fusion neutrons dN/dt is given by

$$\frac{dN(t)}{dt} = \frac{1}{2}A\lambda_f n_{dd}(t), \quad (11)$$

where A is an absolute factor (proportional to the muon

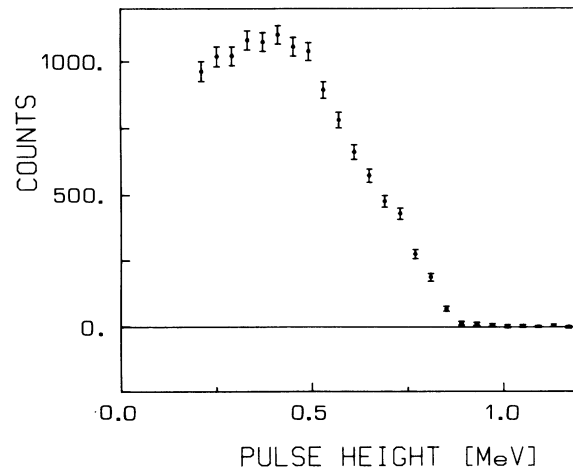


FIG. 8. Experimental proton recoil spectrum due to fusion neutrons ($0.6 < T_{\mu n} < 5 \mu s$). Pulse height axis is calibrated in equivalent electron energy.

stops in deuterium and the overall neutron detection efficiency). Using $\lambda_f \gg c\lambda_d^{\mu d}, c\lambda_{dd}^F, \lambda_0$ expression (11) is essentially simplified:

$$\frac{dN(t)}{dt} = \frac{1}{2}A(c\lambda_{dd}^{1/2}n_{1/2} + c\lambda_{dd}^{3/2}n_{3/2}). \quad (12)$$

In this approximation our qualitative interpretation of the observed time dependent of fusion neutrons becomes evident: The yield of fusion neutrons is a superposition of two components, which clearly show the time evolution of the μd hf population (compare Fig. 9).

To test our explanation the numerical solution of Eq. (10) was used to fit the time spectra of all runs in the range $0.6 < t < 5 \mu\text{s}$. From this fit it was possible to extract the parameters $\lambda_d^{\mu d}$ and $\lambda_{dd}^{3/2}/\lambda_{dd}^{1/2}$ without depending on an absolute normalization [numerical calculations as well as analytical approximations of Eq. (10) show, that $dN(t)/dt$ is nearly insensitive to the absolute value of λ_{dd}^F , if $\lambda_d^{\mu d} \gg \lambda_{dd}^{3/2}$ and $\lambda_0 \gg c\lambda_{dd}^{1/2}$]. The results of this analysis are summarized in Table III, the calculated curves are displayed in Fig. 7. All densities are consistently fit by one set of values $\lambda_d^{\mu d}$ and $\lambda_{dd}^{3/2}/\lambda_{dd}^{1/2}$.

For the determination of the final results only data of the 4.8% run were used, which has the smallest fit errors (Table III) and also the least sensitivity to systematic effects (Table IV). It should be noted in Table IV, that the consideration of a finite slowing down time t_a of the μd atoms (to an energy where hf transitions become irreversible) not only increases the overall errors, but leads to a systematic shift of the $\lambda_{dd}^{3/2}/\lambda_{dd}^{1/2}$ ratio. t_a cannot be extracted from the measurements at different densities because the correction depends on the density independent ratio of the elastic to the inelastic (hf transition) cross sections. Therefore, t_a was estimated to be 25 ± 25 ns at 5% density by direct calculation⁸ and by comparison with the Monte Carlo results of Matone³¹ for hydrogen.

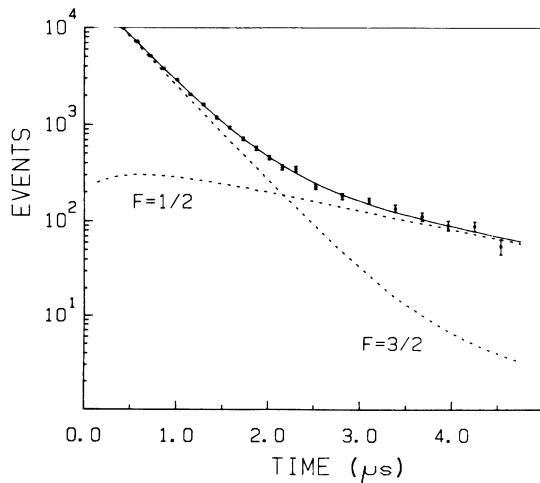


FIG. 9. Time spectrum of fusion neutron after muon stop (density 4.8% of c_0 , bin width $0.144 \mu\text{s}$). According to approximation (12) the calculated time distribution (solid curve, parameters from Table III) is a superposition of two components, corresponding to the $F = \frac{3}{2}$ and $F = \frac{1}{2}$ μd state, respectively.

V. RESULTS AND DISCUSSION

The final results for the ratio of the molecular formation rates and the value for the hyperfine transition rate were determined from the measurement at 4.8% liquid hydrogen density and 34.7 K:

$$\begin{aligned} \lambda_{dd}^{3/2}/\lambda_{dd}^{1/2} &= 79.5 \pm 8.0, \\ \lambda_d^{\mu d} &= (37.0_{-1.7}^{+1.3}) \times 10^6 \end{aligned} \quad (13)$$

(in units of s^{-1} and normalized to liquid-hydrogen density $4.2 \times 10^{22} \text{ cm}^{-3}$), and

$$\lambda_d^{\mu d} = (42.6_{-1.5}^{+1.5}) \times 10^6$$

(in units of s^{-1} and normalized to liquid-deuterium density $4.84 \times 10^{22} \text{ cm}^{-3}$)³² (errors correspond to one standard deviation).

A. Hyperfine transition

Our experiment yields the first accurate experimental result for $\lambda_d^{\mu d}$. It was obtained by a new technique which was not considered before and is independent of the ambiguities of some of the earlier experiments. (For a summary of all published experimental values of $\lambda_d^{\mu d}$ see Table I.) Our experimental value for $\lambda_d^{\mu d}$ allows a clear decision between theoretical results, as it only agrees with Refs. 18 and 19. Our work obviously disagrees with experiment,¹⁵ which reports an upper limit of $15 \times 10^6 \text{ s}^{-1}$ for $\lambda_d^{\mu d}$ with 90% confidence level. Correcting for the higher temperature of the latter experiment³³ does not solve this discrepancy. Whether this disagreement results from unexpected effects showing up at thermal energies equal to the hf splitting energy or is due to systematic problems associated with the indirect and less sensitive method of the Dubna experiment, should be further investigated. Concerning the remaining experimental information it is remarkable that our value is in accordance with the limits given in all other experiments if our recent analysis of liquid target experiments is used (these corrected results are given in the third column of Table I). Moreover, combining these latter experiments in H-D mixtures with our new result for $\lambda_d^{\mu d}$, even a value for $\lambda_p^{\mu d}$ [Eq. (4)] can be determined.³⁴ Thus the long missing experimental information about the hf population of μd atoms (at least at low temperatures) is provided not only for pure D_2 , but also for H-D mixtures. In addition we want to emphasize that the precision of the measured hf transition rate exceeds all previous experimental data on low-energy scattering (elastic and inelastic) of μd atoms by one order of magnitude (Table I and Ref. 10). (The close connection between elastic and inelastic processes is most evident in the scattering length approximation, which is valid at energies of some meV.¹⁸) The measurements were performed at thermal equilibrium of the μd atoms with energies negligible to the hf splitting. Therefore, it is now possible for the first time, to test experimentally the formalism of muonic three-body scattering calculations with about 5% accuracy. For such a quantitative comparison at the moment a detailed theoretical calculation of $\lambda_d^{\mu d}$ is missing that also would include the structure of the scattering D_2 molecule.

TABLE III. Results from the fit of neutron time spectra with fixed $\lambda_{dd}^{1/2}=0.04\times 10^6\text{ s}^{-1}$ (three fit parameters: $\lambda_d^{\mu d}$, $\lambda_{dd}^{3/2}/\lambda_{dd}^{1/2}$, and normalization factor, 18 degrees of freedom). No systematic errors were included.

Density (% of c_0)	χ^2	$\lambda_d^{\mu d}$ (10^6 s^{-1})	$\lambda_{dd}^{3/2}/\lambda_{dd}^{1/2}$	Events in fit range
~ 9.5	12.3	36.3 ± 1.3	91 ± 10	13 957
~ 4.8	15.6	37.0 ± 0.74	84.5 ± 3.3	22 043
~ 2.4	18.8	37.1 ± 2.6	98.7_{-30}^{+80}	8 176

B. Muon capture in deuterium

The new results for the hyperfine transition rates $\lambda_d^{\mu d}$ and $\lambda_p^{\mu d}$ (Ref. 34) strongly differ from the assumptions used in the analyses of the two existing experiments⁴ of reaction (1), which were performed in H-D mixtures. A preliminary reanalysis³ of these experiments indicates considerable changes in the extracted capture rate of the $F=\frac{1}{2}$ μd atom, which lead to a striking discrepancy between the experimental results. Moreover, our detailed understanding of mesomolecular processes in pure deuterium suggests more direct approach to μd capture: Experiments in pure deuterium targets are under way at the moment.³⁵

C. Molecular $d\mu d$ formation

As regards the molecular formation process the pronounced spin dependence discovered in our experiment is a new effect not considered in earlier theoretical work nor observed in previous experiments. We proposed⁹ an explanation on the basis of the resonance mechanism discussed in Sec. IIB additionally assuming molecular formation from both hyperfine states of the μd atom. The formation of the $d\mu d$ molecule in a definite energy state is then characterized by two resonance energies $\epsilon_0(F)$ corresponding to each of the hyperfine states of the atom. The

hyperfine splitting E_{hf} determines the difference between the resonance energies.

$$\epsilon_0(F=\frac{1}{2})-\epsilon_0(F=\frac{3}{2})=E_{\text{hf}}. \quad (14)$$

Thus a resonance close to 34 K (about 4.5 meV) for the $F=\frac{3}{2}$ hf state discovered in our experiment corresponds to a resonance energy around 53 meV for the $F=\frac{1}{2}$ state. Therefore, the resonant process found in Ref. 5 at ~ 400 K can be interpreted as mainly due to molecular formation from the atomic $F=\frac{1}{2}$ state. This interpretation also agrees with the population of the hyperfine states determined in our experiment.

In our analysis charge symmetry has been assumed between the two channels of the dd fusion reaction [Eq. (8)]. However, calculations²⁴ estimate a charge symmetry violation of about 20% in the p wave of this reaction. Because the $J=1$ rotational $d\mu d$ states are populated differently in the resonant and the nonresonant $d\mu d$ formation process, this leads to a peculiar effect: The branching ratio between the dd fusion channels may be different after $d\mu d$ formation from the $F=\frac{1}{2}$ and $F=\frac{3}{2}$ state, respectively. At a temperature of 34 K, for instance, the formation from the $F=\frac{3}{2}$ state is resonant, whereas the formation from the $F=\frac{1}{2}$ is nonresonant. Because of the uncertainties in the partial amplitudes of the dd fusion process,²⁴

TABLE IV. Systematic and statistical errors for the run at 4.8% liquid density. The very conservative estimates of the uncertainties associated with the parameters s_{He} , $\lambda_{dd}^{1/2}$, and λ_f demonstrate their small influence on the final results.

Source of error	Uncertainty	Contribution to error of $\lambda_d^{\mu d}$	Contribution to error of $\lambda_{dd}^{3/2}/\lambda_{dd}^{1/2}$
Target density	$\pm 2\%$ of c	$\pm 1.8\%$	
Zero-point shift in time spectrum	± 16 ns	$< 0.5\%$	$\pm 3\%$
Time calibration	$\pm 1\%$	$\pm 1\%$	$\pm 1.5\%$
$s_{\text{He}}=0.14$ (Ref. 30)	$\pm 50\%$	$\pm 1\%$	$\pm 2\%$
$\lambda_{dd}^{1/2}=0.04\times 10^6\text{ s}^{-1}$	$+75\%$ -25%	$+0.9\%$ -2.8%	$\pm 3.7\%$
$\lambda_f\geq 10^8\text{ s}^{-1}$ (Ref. 24)			$< 1.8\%$
Accidentals	$\pm 3\%$	$\pm 1.4\%$	$\pm 3\%$
μd capture neutrons	< 150 events in fit range		$< 3\%$
$t_a=25$ ns	$\pm 100\%$	$< 1\%$	$\pm 6\%$
Error from χ^2 analysis		$\pm 2\%$	$\pm 3.8\%$
$(\sum \sigma^2)^{1/2}$		$+3.6\%$ -4.5%	$\pm 10\%$

this effect was neglected in our final results. An estimate of its influence yields $\lambda_{dd}^{3/2}/\lambda_{dd}^{1/2} \sim 72$ instead of 79.5 (this estimate uses the calculations for nonresonant $d\mu d$ formation⁶ and the probability for neutron emission after fusion in the $d\mu d$ $J=1$ state²⁴).

The discovery of hf resonances in $d\mu d$ molecular formation makes evident that a clear distinction between both hf rates $\lambda_{dd}^{3/2}$ and $\lambda_{dd}^{1/2}$ is necessary. The ratio of $\lambda_{dd}^{3/2}/\lambda_{dd}^{1/2}$ (measured at 34 K in our experiment) can be used to correct the bubble chamber experiment¹³ (about 31 K temperature), which was interpreted disregarding hf effects. Surprisingly, about 40% of the total fusion yield observed in the bubble chamber results from molecular $d\mu d$ formation from the $F = \frac{3}{2}$ state during the first 100 ns. Therefore, the corrected value for $\lambda_{dd}^{1/2}$ lies between 4.5 and 6.3×10^4 s⁻¹ (depending on the assumptions concerning the branching ratios for the dd fusion channels mentioned above). The theoretical value⁶ for nonresonant $d\mu d$ formation at liquid-deuterium temperature is 4×10^4 s⁻¹. [In the analysis of our data, which is not very sensitive to the value of $\lambda_{dd}^{1/2}$, we have used $\lambda_{dd}^{1/2} = (4_{-1}^{+3}) \times 10^4$ s⁻¹ and, thus, have considered all expected values for $\lambda_{dd}^{1/2}$.]

In addition a new, detailed spectroscopy of the $d\mu d$ mesomolecule is developing from this experiment. As the strong hf resonances correspond to transitions between definite hf states, the molecular formation process is sensitive to the hf splitting of the initial μd atom, as well as to the splitting of the final molecular $d\mu d$ state ($J=1, \nu=1$). Therefore, the measurement of the resonance dependence of λ_{dd}^F will ultimately lead to an accurate determination of the ϵ_{11} level and beyond that can also reveal the hf structure of this state. A first comparison with theory became possible soon after our experiments, when Bakalov *et al.* published the hf structure of the $d\mu d$ molecule in 1980.³⁶ Using the calculated level scheme of the $J=1, \nu=1$ mesomolecular state (and disregarding additional, small sub-splitting) two final $d\mu d$ hf levels can be identified, characterized by the total spin $S = \frac{1}{2}$ and $S = \frac{3}{2}$, respectively. For each of the μd atom hf states (spin F) two transitions for resonant molecular formation are possible (compare Fig. 10). With the help of the populations $W^S(F)$ of the hf sublevels of the mesic molecule (calculated in Ref. 36), one ends up with a formula for the resonant part of λ_{dd}^F

$$\lambda_{dd}^F = \sum W^S(F) \lambda_{dd}(\epsilon_0^S(F)), \quad S = \frac{1}{2}, \frac{3}{2}. \quad (15)$$

Thus each hf component λ_{dd}^F is a superposition of two contributions of the resonance form given in Ref. 6, corresponding to two different resonance energies $\epsilon_0^S(F)$, where $S = \frac{1}{2}, \frac{3}{2}$.

To realize the implications of this refined picture for the accurate determination of the ϵ_{11} energy level, one has to keep in mind that only the resonance energies $\epsilon_0^S(F)$ are directly observable from the temperature dependence of the formation rate. The final state of the $[(d\mu d)dee]$ molecule and thus the value of ϵ_{11} [compare Fig. 1 and Eq. (7)] is fixed by the observed absolute value of the formation rate, because the expected rate depends strongly on the final vibrational level ν .⁶ Regarding the analysis of Refs. 5 and 6 our new interpretation including hf effects [Eq. (15)] leads to a considerable decrease of the expected

absolute rate $\lambda_{dd}^{1/2}$ at 53 meV. (According to our analysis only transition 3, but not transition 4 in Fig. 10 is resonant at that temperature.) A transition to a lower vibrational level ($\nu=7$ instead of $\nu=8$) in the molecular formation process would compensate for this decrease. Such a change in the level scheme of resonant $d\mu d$ formation (Fig. 1) would also imply a large shift of the experimentally determined value of ϵ_{11} by one vibrational quantum, that is ~ 250 meV.

In order to draw definite conclusions, the temperature dependence of the resonant formation rates λ_{dd}^F in the low-temperature region is providing a very promising tool.³⁷ First of all, the absolute temperature spread in the Maxwell distribution is small, which results in a higher sensitivity of the resonance process to small temperature variations. In addition, complications due to higher rotational states of the D_2 molecule (compare Sec. II B) are reduced.

D. Muon induced dt fusion

Finally we want to comment on the significance of our results for muon catalyzed dt fusion.^{6,23,38} Because a similar formation mechanism is proposed for both systems analogous hf effects can also be expected in the $d\mu t$ formation process. In this case the resonance energies for $d\mu t$ formation for the two μt hf states are separated by about 50 meV, corresponding to 387 K (hf structure of $d\mu t$ from Ref. 36). The resulting difference in the resonance behavior of the hf components of the $d\mu t$ formation rate may strongly influence the overall fusion yield in the D-T system (for details see Ref. 38). Concerning the experimental investigations of D-T mixtures it is clear that the determination of the set of parameters describing the kinetics of the $d\mu t$ system gets even tougher if hf effects have to be included. Additional parameters, like the hf

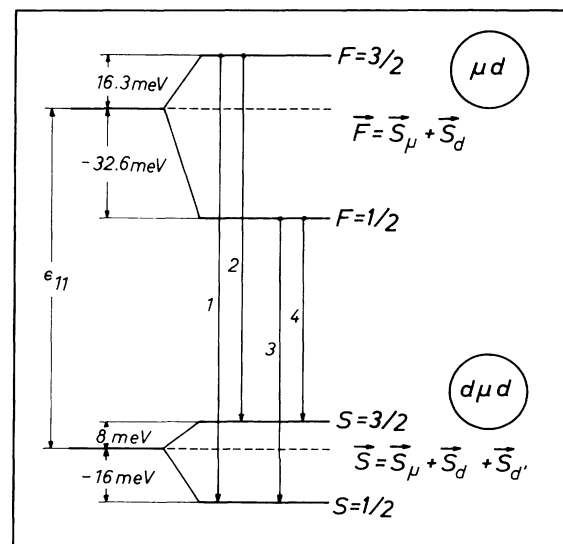


FIG. 10. Hyperfine structure of the μd atom and the $d\mu d$ $J=1, \nu=1$ state (from Ref. 36). Additional splitting is less than 0.5 meV. Transitions, responsible for hf effects in resonant $d\mu d$ formation, are indicated by arrows.

components of the molecular formation rates and the hyperfine transition rates for scattering on deuterium and tritium, then become important. It also should be mentioned that the analysis of the first experiment in a D-T mixture³⁹ was performed disregarding hf effects.

VI. SUMMARY

Owing to improvements in experimental techniques—mainly the high quality of the SIN muon beam and the careful use of a delayed coincidence condition—the first detection of neutrons from muon catalyzed fusion in gaseous deuterium at low temperatures was possible. It showed the first clear-cut experimental evidence for hyperfine effects in pure deuterium. With the help of the strong hyperfine dependence of the formation rate of the $d\mu d$ molecule discovered in this work, the transition between the two hyperfine states of the μd atom was directly manifested for the first time. This method provided the long missing accurate experimental value for the hyperfine transition rate, which determines the μd hyperfine population in pure deuterium.

Concerning experiments on the elementary muon-capture process in deuterium, the detailed knowledge about mesoatomic and mesomolecular processes (μd hyperfine transition and $d\mu d$ molecular formation) obtained in our experiment provides valuable information. For the first time, a clear interpretation of future experiments in pure deuterium is possible.³⁵ This achievement is especially important, because our precise measurement of $\lambda_d^{\mu d}$ (in connection with our earlier experiment¹⁶ on fusion gamma rays in a H-D liquid target) allows a reexamination of the

assumptions about the μd hf populations used in the existing μd capture experiments,⁴ which were performed in H-D mixtures. According to our reanalysis,³⁴ striking discrepancies among these old μd capture experiments now exist.

Regarding our discovery of hyperfine resonances in the $d\mu d$ molecular formation, we are now on the way towards a full quantitative understanding of this process. Our analysis shows that the pronounced hyperfine effects observed in this experiment can consistently be described within the theoretical framework of the resonant formation mechanism.^{6,21} This agreement strongly supports the whole concept of resonant mesomolecular formation. Moreover, our experiment indicates that a refined spectroscopy of muonic molecules capable of determining the energy and even the hyperfine structure of a $d\mu d$ bound state within 1 meV or better, is becoming feasible. Finally we want to emphasize the importance of the detailed consideration of hyperfine effects for cold muon catalyzed dt fusion.

ACKNOWLEDGMENTS

Support by the following institutions enabled these investigations and is gratefully acknowledged: Austrian Academy of Sciences, Austrian Science Foundation, and Swiss Institute for Nuclear Research (SIN). We are indebted to Professor Blaser and Professor Lintner for continuous support and encouragement. Finally, we like to express our gratitude to all the technical services at SIN, whose efficient assistance made this experiment possible.

¹E. Zavattini, in *Muon Physics*, edited by C. S. Wu and V. W. Hughes (Academic, New York, 1975), Vol. II, p. 219.

²W. H. Breunlich, in *Proceedings of the 8th International Conference on High Energy Physics and Nuclear Structure, Vancouver, 1979*, edited by D. F. Measday and A. W. Thomas [Nucl. Phys. **A335**, 137 (1980)].

³W. H. Breunlich, in *Proceedings of the 9th International Conference on the Few Body Problem, Eugene, 1980*, edited by F. S. Levin [Nucl. Phys. **A353**, 201c (1981)].

⁴I. T. Wang, E. W. Anderson, E. J. Bleser, L. M. Lederman, S. L. Meyer, J. L. Rosen, and J. E. Rothberg, Phys. Rev. **139**, 1229 (1965); A. Bertin, A. Vitale, A. Placci, and E. Zavattini, Phys. Rev. D **8**, 3774 (1973).

⁵V. M. Bystritskii, V. P. Dzhelepov, V. I. Petrukhin, A. I. Rudenko, L. N. Somov, V. M. Suvorov, V. V. Fil'chenkov, G. Chemnitz, N. N. Khovanskii, B. A. Khomenko, and D. Horvath, Zh. Eksp. Teor. Fiz. **76**, 460 (1969) [Sov. Phys.—JETP **49**, 232 (1979)].

⁶S. I. Vinitiskii, L. I. Ponomarev, I. V. Puzynin, T. P. Puzynina, L. N. Somov and M. P. Faifman, Zh. Eksp. Teor. Fiz. **74**, 849 (1978) [Sov. Phys.—JETP **47**, 444 (1978)].

⁷Yu. V. Petrov, Nature **285**, 466 (1980).

⁸P. Kammel, Ph.D. thesis, University of Vienna, 1982 (unpublished).

⁹P. Kammel, W. H. Breunlich, M. Cargnelli, H. G. Mahler, J. Zmeskal, W. H. Bertl, C. Petitjean, and W. J. Kossler, Phys. Lett. **112B**, 319 (1982).

¹⁰S. Gershtein and L. I. Ponomarev, in *Muon Physics*, Vol. III, edited by V. Hughes and C. S. Wu (Academic, New York, 1975), p. 141.

¹¹G. Fiorentini, Nucl. Phys. **A374**, 607 (1982); L. Bracci, G. Fiorentini, Phys. Rep. **86**, 171 (1982).

¹²S. S. Gershtein, Zh. Eksp. Teor. Fiz. **40**, 698 (1961) [Sov. Phys.—JETP **13**, 488 (1961)].

¹³J. H. Doede, Phys. Rev. **132**, 1782 (1963).

¹⁴E. J. Bleser, E. W. Anderson, L. M. Lederman, S. L. Meyer, J. L. Rosen, J. E. Rothberg, and I. T. Wang, Phys. Rev. **132**, 2679 (1963).

¹⁵V. M. Bystritskii, V. P. Dzhelepov, V. I. Petrukhin, A. I. Rudenko, V. M. Suvorov, V. V. Fil'chenkov, G. M. Chemnitz, N. N. Khovanskii, and B. A. Khomenko, Zh. Eksp. Teor. Fiz. **71**, 1680 (1976) [Sov. Phys.—JETP **44**, 881 (1976)].

¹⁶H. G. Mahler, W. H. Bertl, W. H. Breunlich, P. Kammel, W. Reiter, C. Petitjean, L. A. Schaller, L. Schellenberg, and W. J. Kossler, *Contribution 1B24 to the 8th International Conference on High Energy Physics and Nuclear Structure, Vancouver, 1979*, edited by D. F. Measday and A. W. Thomas (unpublished). See review talks by E. B. Shera, Nucl. Phys. A **335**, 75 (1980); W. H. Breunlich, *ibid.* **335**, 137 (1980); W. H. Bertl, W. H. Breunlich, P. Kammel, H. G. Mahler, W. Reiter, C. Petitjean, W. J. Kossler, L. A. Schaller, L. Schellenberg, Contribution to the Third International Conference on Emerging Nuclear Energy Systems, Helsinki, 1983 (Atomkernenergie/Kerntechnik, in press).

- ¹⁷V. M. Bystritskii, V. P. Dzhelepov, V. G. Zinov, A. I. Rudenko, L. N. Somov, and V. V. Fil'chenkov, *Zh. Eksp. Teor. Fiz.* **80**, 839 (1981) [*Sov. Phys.—JETP* **53**, 426 (1981)].
- ¹⁸A. V. Matveenko and L. I. Ponomarev, *Zh. Eksp. Teor. Fiz.* **59**, 1593 (1970) [*Sov. Phys.—JETP* **32**, 871 (1971)].
- ¹⁹L. I. Ponomarev, L. N. Somov, and M. I. Faifman, *Yad. Fiz.* **29**, 133 (1979) [*Sov. J. Nucl. Phys.* **29**, 67 (1979)].
- ²⁰A high value of $\lambda_p^{\mu d} \geq 50 \times 10^6 \text{ s}^{-1}$ was first proposed by A. Placci *et al.* to explain the large rate for nuclear muon capture observed in gaseous H-D mixtures [see A. Placci, E. Zavattini, A. Bertin, and A. Vitale, *Phys. Rev. Lett.* **25**, 475 (1970)].
- ²¹E. A. Vesman, *Zh. Eksp. Teor. Fiz. Pis'ma Red.* **5**, 113 (1967) [*JETP Lett.* **5**, 91 (1967)].
- ²²S. I. Vinitskii, V. S. Melezhik, L. I. Ponomarev, I. V. Puzynin, T. P. Puzynina, L. N. Somov, and N. F. Truskova, *Zh. Eksp. Teor. Fiz.* **79**, 698 (1980) [*Sov. Phys.—JETP* **52**, 353 (1980)]; S. I. Vinitskii, V. S. Melezhik, and L. I. Ponomarev, *ibid.* **82**, 670 (1982) [**55**, 400 (1982)].
- ²³S. S. Gershtein, Yu. V. Petrov, L. I. Ponomarev, L. N. Somov, and M. P. Faifman, *Zh. Eksp. Teor. Fiz.* **78**, 2099 (1980) [*Sov. Phys.—JETP* **51**, 1053 (1980)].
- ²⁴L. N. Bogdanova, V. E. Markushin, V. S. Melezhik, and L. I. Ponomarev, *Phys. Lett.* **115B**, 171 (1982).
- ²⁵Reference 8 and J. Marton, W. H. Breunlich, M. Cargnelli, H. Fuhrmann, P. Kammel, P. Pawlek, in *Proceedings of the International Conference on Nuclear Data for Science and Technology, Antwerp, 1982*, edited by K. H. Böckhoff (Reidel, Dordrecht, Holland, 1983).
- ²⁶Pileup Gate GP-100/N, EG&G/ORTEC.
- ²⁷Pulse Shape Discriminator PSD-5010, Link Systems, High Wycombe, England.
- ²⁸A delayed hardware coincidence was already used for investigations on muon catalyzed *pd* fusion (Ref. 14).
- ²⁹This comment also applies to the recent Dubna *dμt* experiment³⁹ where a coincidence was used disregarding this effect.
- ³⁰S. S. Gershtein, Yu. V. Petrov, L. I. Ponomarev, N. P. Popov, L. P. Presnyakov, and L. N. Somov, *Zh. Eksp. Teor. Fiz.* **80**, 1690 (1981) [*Sov. Phys.—JETP* **53**, 872 (1981)].
- ³¹G. Matone, *Nuovo Cimento Lett.* **2**, 151 (1971).
- ³²This value for $\lambda_d^{\mu d}$ coincides with the result given in our previous works (Refs. 3, 8, and 9) where $\lambda_d^{\mu d}$ was normalized to liquid-deuterium density.
- ³³Theoretical temperature dependence from Ref. 18.
- ³⁴For preliminary values compare Refs. 3 and 16.
- ³⁵Measurements in gaseous deuterium performed by our group at SIN. Measurements in liquid deuterium: G. Bardin, J. Duclos, A. Magnon, J. Martino, A. Bertin, M. Capponi, M. Piccinini, and A. Vitale, Contribution M31 to the 9th International Conference on High Energy Physics and Nuclear Structure, Versailles, 1981 (unpublished).
- ³⁶D. D. Bakalov, S. I. Vinitskii, and V. S. Melezhik, *Zh. Eksp. Teor. Fiz.* **79**, 1629 (1980) [*Sov. Phys. JETP* **52**, 820 (1980)].
- ³⁷The temperature dependence of λ_{dd}^F between 25 and 150 K was measured by our group in 1980. For preliminary results see J. Zmeskal, W. H. Breunlich, M. Cargnelli, P. Kammel, J. Marton, P. Pawlek, J. Werner, W. H. Bertl, C. Petitjean, Contribution to the Third International Conference on Emerging Nuclear Energy Systems, Helsinki, 1983 (Atomkernenergie/Kerntechnik, in press).
- ³⁸P. Kammel, J. Werner, W. H. Breunlich, M. Cargnelli, H. Fuhrmann, J. Marton, P. Pawlek, J. Zmeskal, Contribution to the Third International Conference on Emerging Nuclear Energy Systems, Helsinki, 1983 (Atomkernenergie/Kerntechnik, in press).
- ³⁹V. M. Bystritskii, V. P. Dzhelepov, Z. V. Ershova, V. G. Zinov, V. K. Kapyshev, S. Sh. Mukhamet-Galeeva, V. S. Nadezhdin, L. A. Rivkis, A. I. Rudenko, V. I. Satarov, N. V. Sergeeva, L. N. Somov, V. A. Stolupin, and V. V. Fil'chenkov, *Zh. Eksp. Teor. Fiz.* **80**, 1700 (1981) [*Sov. Phys.—JETP* **53**, 877 (1981)].